

Expression and Purification of Functional Ligand–Binding Domains of T1R3 Taste Receptors

Yiling Nie^{1,2}, Jeanette R. Hobbs³, Stephan Vignes¹, Wendy J. Olson¹, Graeme L. Conn³ and Steven D. Munger¹

¹Department of Anatomy and Neurobiology and Graduate Programs in Life Sciences, University of Maryland School of Medicine, Baltimore, MD 21201, USA and

³Faculty of Life Sciences, University of Manchester, Manchester, M60 1QD, UK

²Present address: Department of Physiology, University of California, Los Angeles, Rm 6720 MacDonald Research Laboratories, 675 Charles E. Young Drive South, Los Angeles, CA 90095, USA

Correspondence to be sent to: Steven D. Munger, Department of Anatomy and Neurobiology, University of Maryland School of Medicine, Baltimore, MD 21201, USA. e-mail: smung001@umaryland.edu

Abstract

Chemosensory receptors, including odor, taste, and vomeronasal receptors, comprise the largest group of G protein–coupled receptors (GPCRs) in the mammalian genome. However, little is known about the molecular determinants that are critical for the detection and discrimination of ligands by most of these receptors. This dearth of understanding is due in part to difficulties in preparing functional receptors suitable for biochemical and biophysical analyses. Here we describe in detail two strategies for the expression and purification of the ligand-binding domain of T1R taste receptors, which are constituents of the sweet and umami taste receptors. These class C GPCRs contain a large extracellular N-terminal domain (NTD) that is the site of interaction with most ligands and that is amenable to expression as a separate polypeptide in heterologous cells. The NTD of mouse T1R3 was expressed as two distinct fusion proteins in *Escherichia coli* and purified by column chromatography. Spectroscopic analysis of the purified NTD proteins shows them to be properly folded and capable of binding ligands. This methodology should not only facilitate the characterization of T1R ligand interactions but may also be useful for dissecting the function of other class C GPCRs such as the large family of orphan V2R vomeronasal receptors.

Key words: G protein–coupled receptor (GPCR), protein expression, sugar, sweet taste, T1R3, umami taste

Introduction

Chemosensory receptors detect a diverse array of chemical cues from ions and small organic molecules to peptides and proteins. Despite their importance, however, little progress has been made toward understanding the structural basis of ligand selectivity for these proteins. Most mammalian odor, vomeronasal, and taste receptors are members of the superfamily of G protein–coupled receptors (GPCRs) (Mombaerts, 2004) and share a common seven transmembrane domain motif. Though GPCRs represent the largest mammalian gene family, with thousands of members, only a relative few have been characterized in regards to the molecular determinants of ligand specificity, and crystal structures have been solved for only two, rhodopsin (Palczewski *et al.*, 2000) and the ligand-binding domain of metabotropic glutamate receptor 1 (mGluR1) (Kunishima *et al.*, 2000).

This lack of progress is largely due to the difficulty in obtaining large amounts of purified receptor proteins suitable for biochemical or structural studies. For example, receptor proteins outside the hydrophobic environment of their native lipid membrane may not maintain their normal tertiary structure.

There have been a number of additional hurdles for the structural study of mammalian chemosensory receptors. Isolation of single chemosensory receptor isoforms from native tissue is often infeasible. For example, olfactory, vomeronasal, and gustatory epithelia express dozens to hundreds of distinct chemosensory receptors, with each individual receptor protein expressed in relatively few cells and at low levels. Purification of functional chemosensory receptor proteins from heterologous expression systems has also been

unsuccessful as chemosensory receptors express poorly in heterologous cells, even in the presence of chaperone proteins (Gimelbrant *et al.*, 2001; Mombaerts 2004; Saito *et al.*, 2004). However, we have now overcome many of these difficulties for one group of chemosensory receptors, the T1R taste receptors.

T1R2:T1R3 heteromeric receptors function as a broadly tuned sweet taste receptor, responding to natural sugars, synthetic sweeteners, sweet proteins, and D-amino acids (Nelson *et al.*, 2001; Li *et al.*, 2002; Xu *et al.*, 2004). T1Rs are homologous to other class C GPCRs, including metabotropic glutamate receptors, γ -aminobutyric acid receptors, and Ca^{2+} -sensing receptors, with which they share several structural similarities including a long extracellular N-terminal domain (NTD) that contains the primary ligand-binding site (e.g., Pin *et al.*, 2003; Luu *et al.*, 2004; Morini *et al.*, 2005; Nie *et al.*, 2005). We have taken advantage of this feature to design and execute a strategy for the expression and purification of functional T1R ligand-binding domains.

We previously reported that T1R2NTD and T1R3NTD bind sugars and undergo ligand-dependent conformational changes (Nie *et al.*, 2005). Here we extend those studies to report detailed strategies for obtaining T1R3NTD proteins from bacterial expression systems. Using synchrotron radiation circular dichroism (SRCD) spectroscopy and steady-state fluorescence spectroscopy, we characterize the folding and stability of the expressed proteins and demonstrate their functional interactions with ligands. These studies offer important new analyses of experimental strategies for measuring ligand interactions with chemosensory receptors that should provide new insights into the molecular determinants of ligand specificity and sensitivity across species and receptor variants.

Materials and methods

Generation of expression constructs

We expressed a partial cDNA representing nucleotides 79–1503 of the C57BL/6J allele of mouse *Tlr3* (GenBank accession no. AF337039). This partial cDNA, encoding the amino-terminal domain of the T1R3 protein minus a putative signal sequence and the cysteine-rich domain (e.g., Max *et al.*, 2001), was polymerase chain reaction amplified from clone pCR4TOPot1r3 (a gracious gift from Linda Buck, Fred Hutchinson Cancer Research Center) with primers A1 (5'-GAA TTC CAT ATG CAG CAA TTC AAG GCA CAA GGG-3') and A2 (5'-CTC GAG GAT CTT ATC GTC GTC ATC CTT GTA ATC GTC GAC TGG CAC CTG GTT GCC-3') and inserted into the pGEMT-Easy (Promega, Madison, WI) cloning vector for propagation and sequence confirmation. Primer A2 also encodes an anti-genic FLAG-tag that appears as a C-terminal fusion in the expressed proteins but was not otherwise used in these studies. A silent mutation was introduced to disrupt an endogenous

XhoI site (at nucleotide position 1332), using primers A3 (5'-TGA GTT TCC ATG CAC GAG ACT TGA CAC-3') and A4 (5'-GTG TCA AGT CTC GTG CAT GGA AAC TCA-3') and the QuikChange site-directed mutagenesis kit (Stratagene, La Jolla, CA) to facilitate cloning. This *Tlr3* cDNA fragment (*Tlr3ntd*) was digested with *NdeI* and *XhoI* and ligated into the IMPACT expression vector pTXB1 (New England Biolabs, Ipswich, MA) for isopropyl-beta-D-thiogalactopyranoside (IPTG) induced protein expression (as T1R3NTD) in BL21-CodonPlus(DE3)-RIL *E. coli* (Stratagene) (Figure 1a).

A second expression construct was generated as follows. A cDNA containing the *malE* gene, encoding the *Escherichia coli* maltose-binding protein (MBP), was amplified from pMYB5 vector (New England Biolabs) and cloned into the pET21a vector (Invitrogen, Carlsbad, CA) between the *NdeI* and *NheI* sites. Multiple stop codons were cloned between the restriction sites *Sall* and *XhoI*. A six histidine (6 \times His) tag was engineered downstream to the Shine–Dalgarno (SD) sequence, using the annealed oligonucleotides A5 (5'-GGT GGT CCC TCT AGA AAT AAT TTT GTT TAA C-3') and A6 (5'-CAT ATG GTG GTG GTG GTG GTG GTG CAT TAT ATC TCC TTC TTA AAG-3') to replace the SD sequence in pET21a between the *XbaI* and *NdeI* sites. A flexible linker (encoding 16 amino acids) was cloned in

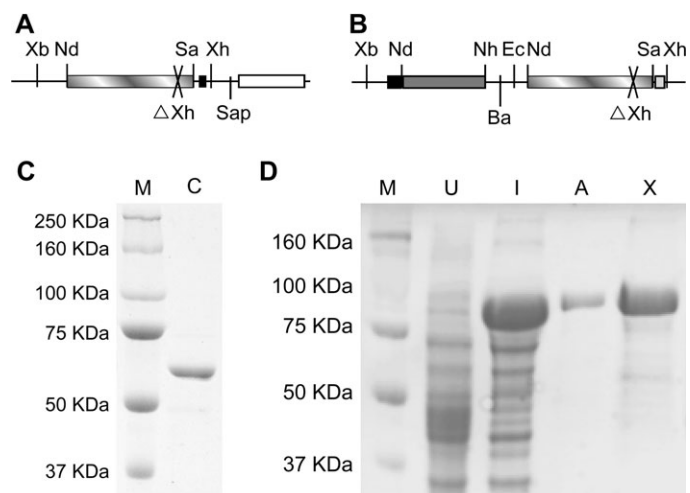


Figure 1 Expression of T1R3NTD as intein–CBD and MBP fusions. **(A)** Expression construct for T1R3NTD (striped box) with a Flag-tag (black box) and intein–CBD fusion at the 3' end. Xb, *XbaI*; Nd, *NdeI*; Sa, *Sall*; Xh, *XhoI*; Δ Xh, deleted *XhoI*; Sap, *SapI*. **(B)** Expression construct for T1R3NTD (striped box) with a 6-histidine tag (black box) and *MalE* (dark gray box) fusion at the 5' end and stop codon introduced at the C-terminal (light gray box). Nh, *NheI*; Ba, *BamHI*; Ec, *EcoRI*. **(C)** Purified T1R3NTD, separated by SDS-PAGE and stained with Coomassie blue; M, molecular weight markers (in kDa); and C, protein fraction eluted from chitin column. From Nie *et al.* (2005), with permission. **(D)** Purified MBP–T1R3NTD, separated by SDS-PAGE and stained with Coomassie blue; M, molecular weight markers (in kDa); U, uninduced cell lysate; I, cell lysate after 3-h induction with 0.5 mM IPTG at 37°C; A, protein fraction after elution from the amylose column; and X, protein fraction after elution from anion exchange column.

between sites *NheI* and *BamHI* sites. Finally, the *T1r3ntd* cDNA (see above) was inserted between restriction enzyme sites *EcoRI* and *SalI* to generate the full expression construct (Figure 1b). This protein was expressed (as MBP-T1R3NTD) after IPTG induction in BL21-CodonPlus(DE3)-RIL *E. coli* (Stratagene).

Expression of T1R3NTD and MBP-T1R3NTD proteins

For T1R3NTD, a single colony of BL21-CodonPlus(DE3)-RIL *E. coli* containing the expression vector was inoculated into 50 ml of Luria-Bertani (LB) broth with 50 µg/ml ampicillin and incubated at 37°C with shaking at 250 rpm overnight. Each liter of LB medium with 50 µg/ml ampicillin was inoculated with 10 ml of the overnight starter culture. IPTG was added to a final concentration of 0.2 mM when the OD₆₀₀ reached 1.0. Induction was performed at 37°C for 1 h with shaking at 250 rpm. Culture was cooled on ice, and then cells were harvested by centrifuging at 5000 × *g* for 15 min at 4°C. Supernatant was decanted, and the weight of pellet was determined (typical yields were approximately 20 g per 8 l culture). Harvested cells were frozen at -20°C for later use. MBP-T1R3NTD was similarly expressed, with the following changes: the culture was induced when the OD₆₀₀ reached 0.6, at which point IPTG was added to a final concentration of 0.5 mM, and the length of induction was 3 h.

Purification of T1R3NTD and MBP-T1R3NTD proteins

T1R3NTD was purified by chitin affinity chromatography using the IMPACT-CN system (New England Biolabs). For 20 g of cell paste, 120 ml of ice-cold cell lysis buffer [20 mM 4-2-hydroxyethyl-1-piperazine ethanesulfonic acid (HEPES)-Na, pH 8.0, 500 mM NaCl, 1 mM ethylenediaminetetraacetic acid (EDTA), 0.5% (v/v) Triton X-100, 0.2% (v/v) Tween-20] was added to resuspend the cells. Phenylmethylsulfonyl fluoride (PMSF), a protease inhibitor, was added to a final concentration of 0.5 mM. Cells were lysed by sonicating 10 times for 40 s each at 4°C, and the lysate was cleared by centrifugation at 5000 × *g* for 30 min. The supernatant was decanted and centrifuged at 20,000 × *g* for 40 min. The supernatant was saved at 4°C until loading. The column containing 2.5 ml of chitin resin (New England Biolabs) was pre-equilibrated with 10 ml of chitin column buffer (20 mM HEPES-Na, pH 8.0, 500 mM NaCl, 1 mM EDTA). The clarified lysate was loaded onto the chitin column at a flow rate of 0.5 ml/min, and the resin was washed extensively with 100 ml of chitin column wash buffer [20 mM HEPES-Na, pH 8.0, 1 M NaCl, 1 mM EDTA, 0.2% (v/v) Triton X-100] followed by 30 ml of chitin column buffer. Chitin column buffer containing 50 mM dithiothreitol (DTT) was added (7.5 ml) and flushed quickly through the chitin column with the eluant collected in 1 ml fractions. Flow was stopped and the chitin resin was incubated at room temperature for 16 h to cleave the T1R3NTD proteins from the fusion tag. T1R3NTD proteins were eluted with additional chitin column buffer

(no DTT) and collected in 1 ml fractions. Protein-containing fractions [as determined by sodium dodecyl sulfate-polyacrylamide gel electrophoresis (SDS-PAGE) analysis] were pooled, concentrated with a Centricon-YM30 (Millipore, Billerica, MA), and dialyzed exhaustively into circular dichroism (CD) buffer (10 mM sodium phosphate, pH 8.0, 150 mM NaF). Protein concentrations were determined by Bradford assay (BioRad, Hercules, CA), and purity was checked through SDS-PAGE analysis (stained by Coomassie brilliant blue 0.1%).

MBP-T1R3NTD was purified by amylose affinity chromatography followed by anion exchange chromatography. For each gram of cells, 3 ml of ice-cold cell lysis buffer I [50 mM Tris-HCl, pH 8.0, 500 mM NaCl, 1 mM EDTA, 0.5% (v/v) Triton X-100, 0.2% (v/v) Tween-20] was added to resuspend the cells, and PMSF was added to a final concentration of 0.5 mM. Resuspended cells were sonicated 10 times for 40 s each at 4°C. The lysate was cleared by centrifugation at 5000 × *g* for 30 min and, of the resulting supernatant, at 20,000 × *g* for 40 min at 4°C. The final supernatant was saved at 4°C. Five milliliters of amylose resin (New England Biolabs) was washed with 8 column volumes of amylose column buffer (20 mM Tris-HCl, pH 8.0, 200 mM NaCl, 1 mM EDTA) before loading the supernatant at a flow rate of 0.5 ml/min. The amylose column was washed with 12 column volumes of amylose column buffer, and the MBP-T1R3NTD core protein was eluted with amylose column elution buffer (20 mM Tris-HCl, pH 8.0, 200 mM NaCl, 1 mM EDTA, 10 mM maltose). Eluant was collected in 1 ml fractions. Protein-containing fractions were diluted fourfold with Q column buffer (20 mM Tris-HCl, pH 8.0) to lower the salt concentration to 50 mM NaCl. The diluted sample was loaded onto one 5 ml HiTrap Q HP column (Amersham Biosciences, Piscataway, NJ) that was pre-equilibrated with 5–10 volume of Q column start buffer A (20 mM Tris-HCl, pH 8.0, 50 mM NaCl) at a flow rate of 5 ml/min on fast protein liquid chromatography (FPLC, ÄKTAprime FPLC system, Amersham Biosciences). After washing with 50 ml of Q column start buffer A, the MBP-T1R3NTD was eluted with a linear NaCl gradient (0.05–1 M NaCl) over 100 ml of 0–100% B (Q column elute buffer B: 20 mM Tris-HCl, pH 8.0, 1M NaCl) and 2.5 ml fractions collected. The MBP-T1R3NTD protein was eluted with 38–45% buffer B. The purified protein was dialyzed into CD buffer, and concentration and purity was determined as for T1R3NTD.

SRCD spectroscopy

SRCD spectroscopy was conducted on beamline 12.1 (MBP-T1R3NTD) at the Synchrotron Radiation Source (SRS), Centre for Protein and Membrane Structure and Dynamics, Daresbury Laboratories (Warrington, UK) and on beamline U11 (T1R3NTD) at the National Synchrotron Light Source (NSLS) at Brookhaven National Laboratory (New York, NY). Spectra were recorded at 1–10 mg/ml protein concentration. For MBP-T1R3NTD, scanning parameters were a 0.01 cm path length quartz cell, scanning wavelengths from

260 to 180 nm, bandwidth of 0.5 nm, digital integration time of 5 s, time constant of 1 s, step size of 1 nm, and sensitivity of 50 μ V. For T1R3NTD, scanning parameters were a 0.001-cm path length quartz cell, scanning wavelengths from 260 to 170 nm, bandwidth of 0.5 nm, digital integration time of 1 s, time constant of 200 ms, step size of 1 nm, and sensitivity of 200 μ V. SRCD data were collected as raw absorbance units (ΔA) and were converted to ellipticity (Θ , in mdeg) and then adjusted for sample concentration and converted to a standard unit according to equations (1) and (2):

$$\Delta A = \frac{[\Theta]}{32980}, \quad (1)$$

$$[\Theta]_{\text{mrw}} = \frac{\Theta \times M_{\text{mrw}}}{[10 \times c \times l]}, \quad (2)$$

where c is the protein concentration (in mg/ml), l is the cell path length in centimeters, and M_{mrw} is the mean residue molecular weight. The dimensions of $[\Theta]_{\text{mrw}}$ are $\text{deg}\cdot\text{cm}^2/\text{dmol}$, and the quantity is independent of molecular weight. Each spectrum is the average of three to six individual scans collected on at least two separate samples.

The secondary structure content of the proteins was analyzed based on the Chou and Fasman protein database (Chen *et al.*, 1974). Spectra were deconvoluted using CDNN software and deconvolution algorithms on DICHROWEB (<http://www.cryst.bbk.ac.uk/cdweb/html>) (Lobley, 2001; Whitmore and Wallace, 2004) to compare the obtained SRCD spectra to those of characterized proteins.

Steady-state fluorescence measurements

The intrinsic fluorescence of MBP-T1R3NTD or T1R3NTD was measured using a Jasco FP-6500 fluorescence spectrometer (Easton, MD) equipped with a stirrer and a Peltier temperature-controlled 3 ml, 10 mm path length quartz cuvette. Protein samples, at 200–500 nM, were held at 25°C and excited at 295 nm; emission spectra were recorded from 300 nm (3-nm bandwidth) to 420 nm (3-nm bandwidth) before and after denaturation with 8 M urea. For ligand titration experiments, the peak emission wavelength, which was determined in pilot experiments, was recorded after each titration. Ligand solutions were prepared using the final dialysis buffer. Fluorescence measurements were corrected for bleaching and nonspecific buffer quenching. The K_d values of ligand–receptor interactions were determined using equation (3):

$$\frac{\Delta F}{\Delta F_{\text{max}}} = \frac{[L]_{\text{tot}}}{(K_d + [L]_{\text{tot}})}, \quad (3)$$

where K_d is the apparent dissociation constant, ΔF is the magnitude of the difference between the fluorescence intensity in the absence of ligand and the observed fluorescence intensity at a given concentration of ligand, and ΔF_{max} is that difference at infinite $[L]$. Best-fit curves were generated with Origin 7.0 software. Data points were expressed as means \pm

SEMs of at least three experiments conducted with separate samples. Ligand-dependent quenching of the intrinsic tryptophan fluorescence of T1R3NTD has been reported elsewhere (Nie *et al.*, 2005).

Results

Expression and purification of T1R3NTD and MBP-T1R3NTD proteins

To quantify the interaction of sweet ligands with the NTD of T1Rs, it was necessary to design an expression and purification protocol that would permit the isolation of purified, soluble T1R NTD proteins in sufficient quantities for biochemical studies. We took advantage of two bacterial expression strategies to accomplish this goal. In the first, T1R3NTD was expressed as an N-terminal fusion with a mini-intein and chitin-binding domain (CBD) using the IMPACT vector pTXB1 (New England Biolabs) in BL21-CodonPlus(DE3)-RIL *E. coli* (Stratagene) (Figure 1a). After a 1 h induction by IPTG, the bacteria were harvested by centrifugation and lysed by sonication (optimum induction times were empirically determined and varied for each protein). Next, cellular debris was pelleted, and the clarified lysate was loaded onto a gravity-flow column containing a chitin resin. The bound proteins were washed extensively, and the T1R3NTD protein was cleaved from the bound intein–CBD under reducing conditions. After elution, the T1R3NTD protein was quantified by Bradford assay, and its purity was evaluated by SDS-PAGE (Figure 1c). T1R3NTD, which ran as a 53 kDa band, was the dominant portion of the purified fraction. Protein yields were approximately 100 μ g purified T1R3NTD per liter bacterial culture.

We also expressed T1R3NTD as a C-terminal fusion with the *E. coli* MBP using a modified pET21a vector (Invitrogen), again in BL21-CodonPlus(DE3)-RIL *E. coli* (Figure 1b). After a 3 h induction with IPTG, the bacteria were harvested by centrifugation and lysed by sonication. Cellular debris was pelleted, and the clarified lysate was loaded onto a gravity-flow column containing amylose resin. After extensive washing, the bound protein was eluted with maltose. To remove the maltose, which could confound subsequent ligand interaction studies, eluate fractions containing protein were loaded onto an anion exchange column for separation by FPLC. After elution and dialysis of the MBP-T1R3NTD protein, concentration was determined by Bradford assay and its purity evaluated by SDS-PAGE (Figure 1d). MBP-T1R3NTD, which ran as a 90-kDa band, was the dominant portion of the purified fraction. Protein yields were approximately 500 μ g purified MBP-T1R3NTD per liter bacterial culture.

Secondary structure of T1R3NTD and MBP-T1R3NTD

SRCD spectroscopy can be used to characterize the secondary structure content of chiral molecules such as proteins

(Wallace, 2000). To determine if T1R3NTD and MBP-T1R3NTD were properly folded, we obtained the SRCD spectra of these proteins on NSLS beamline U11 (Brookhaven National Laboratory) or SRS beamline 12.1 (Daresbury Laboratory), respectively (Figure 2a,b). Raw absorbance units were converted to mean residue molar ellipticity ($[\Theta]_{\text{mrw}}$) as described in Materials and Methods. Qualitative examination of the spectra indicates that both proteins are well folded. Differences in the spectra reflect the contribution of the large MBP domain of MBP-T1R3NTD. We deconvoluted the SRCD spectra of T1R3NTD (Figure 2a) using tools available through DICHROWEB and calculated that this protein contains an average 47% α -helix, 12% β -sheet, 14% turn, and 22% other structures across all relevant databases. This composition is consistent with that predicted from the primary protein structure and those of other family C GPCR NTDs (Goldsmith *et al.*, 1999; Kunishima *et al.*, 2000), indicating that T1R3NTD is properly folded.

Another characteristic of folded proteins is that chemical denaturation can cause a dramatic shift in both the amount and the peak wavelength of their intrinsic tryptophan fluorescence as these parameters are subject to the microenvironments of each tryptophan. For example, tryptophans within a hydrophobic core display emission maxima at 330 nm or

less, whereas tryptophans localized in more hydrophilic surroundings have an emission peak around 350 nm (Eftink and Ghiron, 1981). We measured the fluorescence spectra of both T1R3NTD and MBP-T1R3NTD upon excitation with 295 nm light. T1R3NTD exhibited an emission maximum at 337 nm, suggesting that tryptophan residues within the protein are localized within a number of microenvironments. Denaturation of T1R3NTD with 8 M urea caused a red shift of the emission maximum to 342 nm and a 13% decrease in fluorescence intensity (Figure 2c), indicating that the protein was folded prior to denaturation. We similarly characterized MBP-T1R3NTD. This protein displayed an emission maximum at 338.5 nm. Denaturation of MBP-T1R3NTD with 8 M urea caused a red shift of the emission maximum to 344 nm and a 41% decrease in fluorescence intensity (Figure 2d), indicating that this protein, like T1R3NTD, is folded and thermodynamically stable in aqueous solution.

Interactions of MBP-T1R3NTD with saccharides

We previously reported that T1R3NTD and an MBP-fused T1R2NTD each bind saccharide ligands with physiologically relevant affinities (Nie *et al.*, 2005). To further validate our expression strategy, we characterized the interactions of

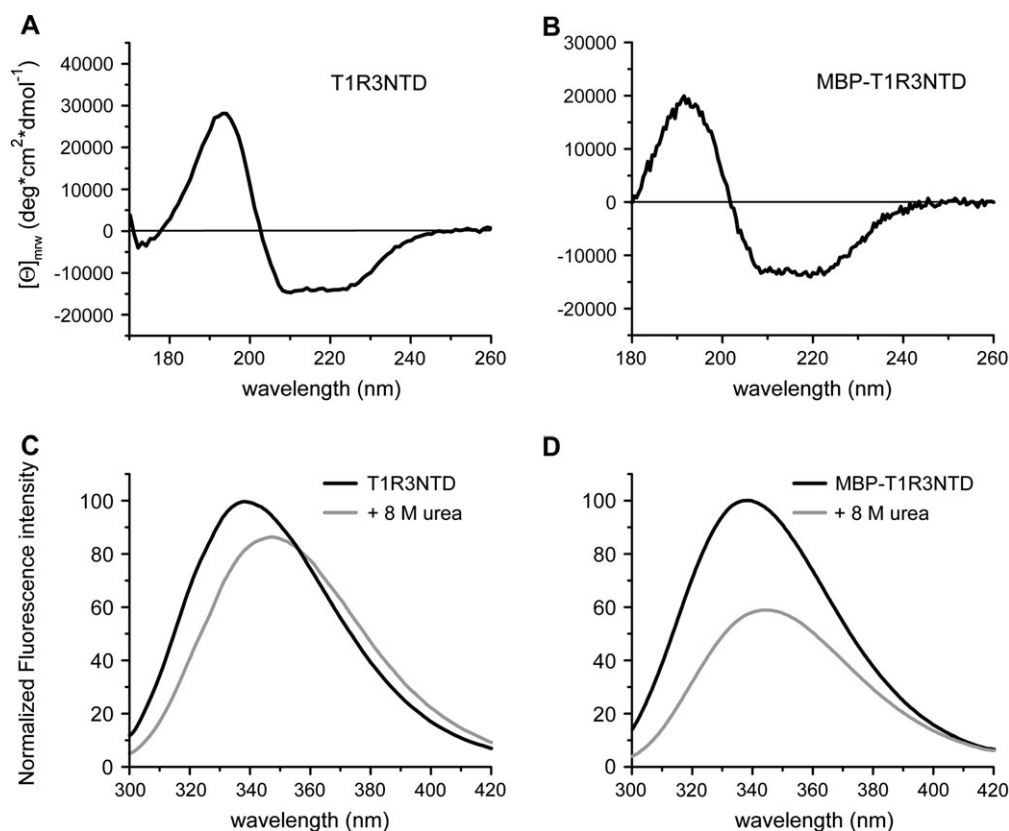


Figure 2 Characterization of T1R3NTD protein folding. **(A)** SRCD spectrum of T1R3NTD. **(B)** SRCD spectrum of MBP-T1R3NTD. **(C)** Intrinsic tryptophan fluorescence spectrum of T1R3NTD in the absence (black) and presence (gray) of 8 M urea. **(D)** Intrinsic tryptophan fluorescence spectrum of MBP-T1R3NTD in the absence (black) and presence (gray) of 8 M urea.

two sugars with MBP-T1R3NTD. First, we determined the concentration–response relationships for the peak intrinsic tryptophan fluorescence of the protein upon titration of glucose or sucrose. Each sugar decreased the peak fluorescence intensity of MBP-T1R3NTD (Figure 3a), exhibiting K_d values of 8.2 ± 1.5 mM and 3.4 ± 0.5 mM for sucrose and glucose, respectively (Figure 3b). Cyclamate, which is perceived as sweet by humans but is not preferred by rodents (Bachmanov *et al.*, 2001) and has been demonstrated to interact with the transmembrane domains of human T1R3 (Xu *et al.*, 2004; Jiang *et al.*, 2005b), had no effect on the intrinsic fluorescence of the mouse MBP-T1R3NTD protein (Figure 3a). These interactions are specific and were not affected by the presence of the MBP fusion (Nie *et al.*, 2005): 1) K_d values of glucose and sucrose interactions with MBP-T1R3NTD were nearly identical from those seen for T1R3NTD and 2) the intrinsic tryptophan fluorescence of MBP alone is quenched by maltose but not by sucrose. The K_d values obtained here are consistent with behavioral studies in mice, where thresholds for sucrose have been found as low as 2 mM (Eylam and Spector, 2004; Glendinning *et al.*, 2005; Delay *et al.*, 2006).

SRCD spectroscopy is sensitive to both the secondary and tertiary structures of proteins (Manavalan and Johnson, 1983; Venyaminov and Vassilenko, 1994; Wallace, 2000). Therefore, SRCD can reveal large conformational changes, such as those that occur upon ligand binding to class C GPCRs (Kunishima *et al.*, 2000; Nie *et al.*, 2005). We obtained the SRCD spectrum of MBP-T1R3NTD in the absence or presence of 5 mM glucose or sucrose (Figure 3c). Both sugars shifted the SRCD spectrum of MBP-T1R3NTD equivalently and in a manner similar to that we previously reported for T1R3NTD (Nie *et al.*, 2005). Once again, these

effects are specific: saccharide-dependent shifts in the spectra of MBP-T1R2NTD are distinct from those shown here, and glucose does not cause a shift in the CD spectrum of MBP itself (Nie *et al.*, 2005).

Discussion

Here we describe the expression and purification of the saccharide-binding domain of the T1R3 sweet taste receptor as a soluble, folded, and functional protein. These studies extend the characterization of T1R NTD proteins previously reported (Nie *et al.*, 2005) to more fully analyze the folding and functionality of the T1R3NTD when heterologously expressed in bacteria.

T1R NTDs offer a number of advantages over intact receptors for dissecting the mechanisms of ligand detection and receptor activation. In standard cell-based assays (e.g., Nelson *et al.*, 2001; Jiang *et al.*, 2004; Xu *et al.*, 2004; Shirokova *et al.*, 2005; Winnig *et al.*, 2005), the efficacy of receptor activation is determined by the ability of the heterologously expressed receptor to couple to a heterotrimeric G protein and to elicit a change in intracellular calcium. Therefore, cell-based assays cannot differentiate the contributions of ligand binding from other aspects of receptor signaling, such as ligand-dependent changes in secondary and/or tertiary structure, intersubunit interactions, or the efficiency of G protein coupling. Each of these steps is critical in the activation of GPCRs by ligands. The NTDs of class C GPCRs each appear to exist as a bilobed, venus flytrap module in equilibrium between open and closed states; ligand binding stabilizes the closed conformation and leads to the activation of the receptor (Kunishima *et al.*, 2000; Pin *et al.*, 2003). Additionally, cooperative interactions

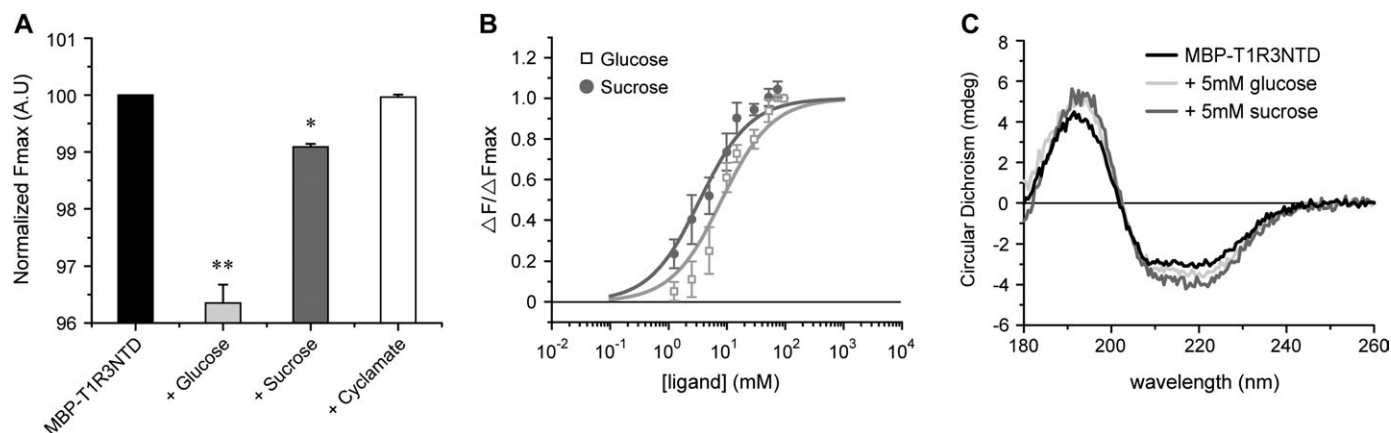


Figure 3 MBP-T1R3NTD binds sugars. **(A)** Normalized maximal fluorescence intensity of MBP-T1R3NTD before and after titration of glucose (final concentration 80 mM; light gray), sucrose (final concentration 80 mM; dark gray), and cyclamate (final concentration 10 mM; white) [(one-way analysis of variance, $F(3,8) = 109$ ($P < 0.0001$); Dunnett's multiple comparison ($*P < 0.05$, $**P < 0.01$)]. **(B)** The intrinsic tryptophan fluorescence intensity of MBP-T1R3NTD was measured as a function of ligand concentration for glucose (open gray square) and sucrose (closed gray circle). The K_d values were 8.2 ± 1.5 mM (glucose) and 3.4 ± 0.5 mM (sucrose). Data from the same experiments are shown in panels (A) and (B); all data points represent means \pm SEMs of six independent experiments. **(C)** SRCD spectra of MBP-T1R3NTD in the absence (black) or presence of glucose (light gray) or sucrose (dark gray). Both ligands cause large shifts in the SRCD spectra at 193 nm (positive shift) and 205–230 nm (negative shift). Cyclamate did not cause a shift in the SRCD spectrum (data not shown).

between subunits of class C GPCR dimers are important for the modulation of ligand binding (Kaupmann *et al.*, 1998; Suzuki *et al.*, 2004) and for coupling the activated receptor to the G protein (Robbins *et al.*, 2001). Comparisons of ligand binding in homomeric and heteromeric mixes of T1R NTDs should further elucidate the contribution of intersubunit interaction in some of these processes. Interestingly, the K_d values we report here and elsewhere are somewhat lower than the EC₅₀s for sugars obtained in behavioral or cell activation assays (Nelson *et al.*, 2001; Eylam and Spector, 2004; Glendinning *et al.*, 2005). This suggests that, as is the case for other GPCRs, ligand affinity and receptor efficacy are not equivalent (Colquhoun, 1998) and that cooperative interactions between subunits along with other processes that contribute to receptor signaling (e.g., G protein coupling) may play important roles in modulating the efficacy of the sweet taste receptor.

Not all T1R ligands bind within the NTDs. Findings by several groups that the sweetener cyclamate and the sweet taste inhibitor lactisole interact with the transmembrane domain of T1R3 (Xu *et al.*, 2004; Jiang *et al.*, 2005a,b; Winnig *et al.*, 2005) begs the question of whether other sweeteners may bind outside the NTDs. This may well be the case, particularly for other synthetic sweeteners. The activation of T1R2:T1R3 receptors by the sweet protein brazzein is dependent on the cysteine-rich region that links the NTD and the transmembrane domain (Jiang *et al.*, 2004), though it is still unclear whether this dependence is due to the presence of a brazzein binding site or to some other aspect of receptor activation. The binding sites for sugars appear to be restricted to the NTDs of T1R2 and T1R3 (Nie *et al.*, 2005).

Escherichia coli expression systems are widely used to express mammalian proteins, displaying well-understood genetics and biochemistry, ease of growth and genetic manipulation, rapid doubling time, and relatively low expense in media or equipment when compared to many eukaryotic expression systems. Bacterial expression systems do not perform some posttranslational modifications of eukaryotic proteins, such as N-linked glycosylation. Glycosylation is critical for membrane trafficking of many GPCRs, but its absence does not appear to interfere with ligand binding (Davidson *et al.*, 1995; Davis *et al.*, 1997). Native T1Rs are likely glycosylated on their NTDs (e.g., Max *et al.*, 2001), though T1R2NTD and T1R3NTD still interact with ligands in the absence of any glycosylation (Figure 3) (Nie *et al.*, 2005). Furthermore, potential changes in glycosylation of T1R3 due to an amino acid change found in mice with reduced sweet taste sensitivity (Max *et al.*, 2001; Reed *et al.*, 2004) do not account for the change in the ligand affinity of T1R3 (Nie *et al.*, 2005). The rarity of T1R proteins in the gustatory epithelium has made the biochemical characterization of native T1Rs extremely difficult. Refined isolation techniques may someday facilitate the analysis of posttranslational modifications of native T1Rs.

We utilized two different strategies to express and purify T1R NTD proteins. Each offered distinct advantages and disadvantages. For the NTD of T1R3, fusion with MBP resulted in an average fivefold greater yield of purified protein than did fusion with the intein-CBD; the NTD of mouse T1R2 has only been successfully expressed as an MBP fusion (Nie *et al.*, 2005). MBP-T1R3NTD was also somewhat more stable in low salt than was T1R3NTD, though this was not so for mouse MBP-T1R2NTD (Nie *et al.*, 2005). However, while the expression of the MBP-fused NTD of T1R3 proteins yields higher levels of expression and stability, purification is more time consuming as it requires two chromatography steps. The presence of the MBP can also needlessly complicate functional analysis of ligand interactions with T1R NTDs as MBP is a sugar-binding protein. Control experiments demonstrating that MBP alone does not interact with the ligands of interest in either SRCD or fluorescence assays (e.g., glucose, sucrose, or sucralose) can rule out non-specific interactions (e.g., Nie *et al.*, 2005) but are consuming of time, reagents, and limited instrument access. Furthermore, the interactions of ligands such as maltose that do bind MBP cannot be accurately determined for the T1Rs using this system.

Fusion of T1R3NTD to the intein-CBD provided for easy purification through a single affinity column, without the retention of either a large fusion protein (e.g., MBP) or the necessity of protease-mediated cleavage of the target protein. However, the use of reducing conditions to release the target protein likely disrupts both inter- and intramolecular disulfide bonds, at least temporarily. This is an important concern: intramolecular disulfide bonds can be critical for maintaining the native three-dimensional structure of proteins (e.g., Cook and Eidne, 1997), while intermolecular disulfide bonds are important for the dimerization of some class C GPCR NTDs (Kunishima *et al.*, 2000). Based on the crystal structure of the mGluR1 NTD, three or four disulfide bonds may exist in the homologous NTD of T1R3 (Max *et al.*, 2001). These disulfide bonds may reform upon dialysis into oxidizing conditions (Zhang *et al.*, 2002). Our SRCD and fluorescence experiments reported here (Figures 2 and 3) and elsewhere (Nie *et al.*, 2005) support this interpretation: they show T1R3NTD to be folded and capable of binding several sweet ligands similarly to MBP-T1R3NTD.

Changes in intrinsic tryptophan fluorescence of T1R NTDs could result from either or both of the two phenomena: ligands may directly quench (or increase) the fluorescence emitted by one or more tryptophan residues in the binding pocket, or the environment of more distant tryptophans might be altered upon ligand-dependent conformational changes. These studies cannot differentiate these two possibilities but are consistent with those for some other class C GPCRs, such as mGluR1 (Suzuki *et al.*, 2004), where ligand binding can be observed through changes in intrinsic tryptophan fluorescence. CD has less commonly been used to measure ligand interactions (e.g., Rodi *et al.*, 1999; Baneres *et al.*,

2005) but promises to be an extremely powerful technique for dissecting conformational changes of receptors and other proteins (Wallace, 2000).

In conclusion, the NTDs of T1Rs can be expressed as soluble proteins that retain ligand-binding functionality. These methods may also be applicable to other class C GPCRs, including the large family of V2R orphan vomeronasal receptors that may play an important role in the detection of MHC peptides (Leinders-Zufall *et al.*, 2004) or other chemosensory stimuli.

Acknowledgements

The authors thank J. Sutherland and J. Trunk for advice on SRCID experiments and L. Buck for providing the T1R3 clone. SRCID experiments were performed on beamline U11 at the NSLS, Brookhaven National Laboratory (supported by the United States Department of Energy) and beamline 12.1 at the SRS, Centre for Protein and Membrane Structure and Dynamics, Daresbury Laboratory (supported by Council for the Central Laboratory of the Research Councils). This work was supported by a grant from the National Institute on Deafness and Other Communication Disorders (NIDCD) (DC05786 to S.D.M.) and fellowship support from The Wellcome Trust (061444 to G.L.C.). W.J.O. was supported by an NIDCD institutional training grant (DC00054).

References

- Bachmanov, A.A., Tordoff, M.G. and Beauchamp, G.K. (2001) Sweetener preference of C57BL/6ByJ and 129P3/J mice. *Chem. Senses*, 26, 905–913.
- Baneres, J.L., Mesnier, D., Martin, A., Joubert, L., Dumuis, A. and Bockaert, J. (2005) Molecular characterization of a purified 5-HT₄ receptor: a structural basis for drug efficacy. *J. Biol. Chem.*, 280, 20253–20260.
- Chen, Y.H., Yang, J.T. and Chau, K.H. (1974) Determination of the helix and beta form of proteins in aqueous solution by circular dichroism. *Biochemistry*, 13, 3350–3359.
- Colquhoun, D. (1998) Binding, gating, affinity and efficacy: the interpretation of structure-activity relationships for agonists and of the effects of mutating receptors. *Br. J. Pharmacol.*, 125, 924–947.
- Cook, J.V. and Eidne, K.A. (1997) An intramolecular disulfide bond between conserved extracellular cysteines in the gonadotropin-releasing hormone receptor is essential for binding and activation. *Endocrinology*, 138, 2800–2806.
- Davidson, J.S., Flanagan, C.A., Zhou, W., Becker, II, Elario, R., Emeran, W., Sealfon, S.C. and Millar, R.P. (1995) Identification of N-glycosylation sites in the gonadotropin-releasing hormone receptor: role in receptor expression but not ligand binding. *Mol. Cell. Endocrinol.*, 107, 241–245.
- Davis, D.P., Rozell, T.G., Liu, X. and Segaloff, D.L. (1997) The six N-linked carbohydrates of the lutropin/choriogonadotropin receptor are not absolutely required for correct folding, cell surface expression, hormone binding, or signal transduction. *Mol. Endocrinol.*, 11, 550–562.
- Delay, E.R., Hernandez, N.P., Bromley, K. and Margolskee, R.F. (2006) Sucrose and monosodium glutamate taste thresholds and discrimination ability of T1R3 knockout mice. *Chem. Senses*, DOI: 10.1093/chemse/bjj039.
- Eftink, M.R. and Ghiron, C.A. (1981) Fluorescence quenching studies with proteins. *Anal. Biochem.*, 114, 199–227.
- Eylam, S. and Spector, A.C. (2004) Stimulus processing of glycine is dissociable from that of sucrose and glucose based on behaviorally measured taste signal detection in Sac 'taster' and 'non-taster' mice. *Chem. Senses*, 29, 639–649.
- Gimelbrant, A.A., Haley, S.L. and McClintock, T.S. (2001) Olfactory receptor trafficking involves conserved regulatory steps. *J. Biol. Chem.*, 276, 7285–7290.
- Glendinning, J.I., Chyou, S., Lin, I., Onishi, M., Patel, P. and Zheng, K.H. (2005) Initial licking responses of mice to sweeteners: effects of *tas1r3* polymorphisms. *Chem. Senses*, 30, 601–614.
- Goldsmith, P.K., Fan, G.F., Ray, K., Shiloach, J., McPhie, P., Rogers, K.V. and Spiegel, A.M. (1999) Expression, purification, and biochemical characterization of the amino-terminal extracellular domain of the human calcium receptor. *J. Biol. Chem.*, 274, 11303–11309.
- Jiang, P., Cui, M., Zhao, B., Liu, Z., Snyder, L.A., Benard, L.M., Osman, R., Margolskee, R.F. and Max, M. (2005a) Lactisole interacts with the transmembrane domains of human T1R3 to inhibit sweet taste. *J. Biol. Chem.*, 280, 15238–15246.
- Jiang, P., Cui, M., Zhao, B., Snyder, L.A., Benard, L.M., Osman, R., Max, M. and Margolskee, R.F. (2005b) Identification of the cyclamate interaction site within the transmembrane domain of the human sweet taste receptor subunit T1R3. *J. Biol. Chem.*, 280, 34296–34305.
- Jiang, P., Ji, Q., Liu, Z., Snyder, L.A., Benard, L.M., Margolskee, R.F. and Max, M. (2004) The cysteine-rich region of T1R3 determines responses to intensely sweet proteins. *J. Biol. Chem.*, 279, 45068–45075.
- Kaupmann, K., Malitschek, B., Schuler, V., Heid, J., Froestl, W., Beck, P., Mosbacher, J., Bischoff, S., Kulik, A., Shigemoto, R., Karschin, A. and Bettler, B. (1998) GABA(B)-receptor subtypes assemble into functional heteromeric complexes. *Nature*, 396, 683–687.
- Kunishima, N., Shimada, Y., Tsuji, Y., Sato, T., Yamamoto, M., Kumasaka, T., Nakanishi, S., Jingami, H. and Morikawa, K. (2000) Structural basis of glutamate recognition by a dimeric metabotropic glutamate receptor. *Nature*, 407, 971–977.
- Leinders-Zufall, T., Brennan, P., Widmayer, P., Chandramani, P.S., Maul-Pavicic, A., Jager, M., Li, X.H., Breer, H., Zufall, F. and Boehm, T. (2004) MHC class I peptides as chemosensory signals in the vomeronasal organ. *Science*, 306, 1033–1037.
- Li, X., Staszewski, L., Xu, H., Durick, K., Zoller, M. and Adler, E. (2002) Human receptors for sweet and umami taste. *Proc. Natl Acad. Sci. USA*, 99, 4692–4696.
- Lobley, A., Whitmore, L. and Wallace, B.A. (2001) DICHROWEB; a website for the analysis of protein secondary structure from circular dichroism spectra. *Biophys. J.*, 80, 373a.
- Luu, P., Acher, F., Bertrand, H.O., Fan, J. and Ngai, J. (2004) Molecular determinants of ligand selectivity in a vertebrate odorant receptor. *J. Neurosci.*, 24, 10128–10137.
- Manavalan, P. and Johnson, W.C. Jr (1983) Sensitivity of circular dichroism to protein tertiary class. *Nature*, 305, 831–832.
- Max, M., Shanker, Y.G., Huang, L., Rong, M., Liu, Z., Campagne, F., Weinstein, H., Damak, S. and Margolskee, R.F. (2001) *Tas1r3*, encoding a new candidate taste receptor, is allelic to the sweet responsiveness locus *Sac*. *Nat. Genet.*, 28, 58–63.
- Mombaerts, P. (2004) Genes and ligands for odorant, vomeronasal and taste receptors. *Nat. Rev. Neurosci.*, 5, 263–278.
- Morini, G., Bassoli, A. and Temussi, P.A. (2005) From small sweeteners to sweet proteins: anatomy of the binding sites of the human T1R2_T1R3 receptor. *J. Med. Chem.*, 48, 5520–5529.
- Nelson, G., Hoon, M.A., Chandrashekar, J., Zhang, Y., Ryba, N.J. and Zuker, C.S. (2001) Mammalian sweet taste receptors. *Cell*, 106, 381–390.

- Nie, Y., Vignes, S., Hobbs, J.R., Conn, G.L. and Munger, S.D. (2005) Distinct contributions of T1R2 and T1R3 taste receptor subunits to the detection of sweet stimuli. *Curr. Biol.*, 15, 1948–1952.
- Palczewski, K., Kumasaka, T., Hori, T., Behnke, C.A., Motoshima, H., Fox, B.A., Le Trong, I., Teller, D.C., Okada, T., Stenkamp, R.E., Yamamoto, M. and Miyano, M. (2000) Crystal structure of rhodopsin: a G protein-coupled receptor. *Science*, 289, 739–745.
- Pin, J.P., Galvez, T. and Prezeau, L. (2003) Evolution, structure, and activation mechanism of family 3/C G-protein-coupled receptors. *Pharmacol. Ther.*, 98, 325–354.
- Reed, D.R., Li, S., Li, X., Huang, L., Tordoff, M.G., Starling-Roney, R., Taniguchi, K., West, D.B., Ohmen, J.D., Beauchamp, G.K. and Bachmanov, A.A. (2004) Polymorphisms in the taste receptor gene (*Tas1r3*) region are associated with saccharin preference in 30 mouse strains. *J. Neurosci.*, 24, 938–946.
- Robbins, M.J., Calver, A.R., Filippov, A.K., Hirst, W.D., Russell, R.B., Wood, M.D., Nasir, S., Couve, A., Brown, D.A., Moss, S.J. and Pangalos, M.N. (2001) GABA(B2) is essential for g-protein coupling of the GABA(B) receptor heterodimer. *J. Neurosci.*, 21, 8043–8052.
- Rodi, D.J., Janes, R.W., Sanganeer, H.J., Holton, R.A., Wallace, B.A. and Makowski, L. (1999) Screening of a library of phage-displayed peptides identifies human bcl-2 as a taxol-binding protein. *J. Mol. Biol.*, 285, 197–203.
- Saito, H., Kubota, M., Roberts, R.W., Chi, Q. and Matsunami, H. (2004) RTP family members induce functional expression of mammalian odorant receptors. *Cell*, 119, 679–691.
- Shirokova, E., Schmiedeberg, K., Bedner, P., Niessen, H., Willecke, K., Raguse, J.D., Meyerhof, W. and Krautwurst, D. (2005) Identification of specific ligands for orphan olfactory receptors. G protein-dependent agonism and antagonism of odorants. *J. Biol. Chem.*, 280, 11807–11815.
- Suzuki, Y., Moriyoshi, E., Tsuchiya, D. and Jingami, H. (2004) Negative cooperativity of glutamate binding in the dimeric metabotropic glutamate receptor subtype 1. *J. Biol. Chem.*, 279, 35526–35534.
- Venjaminov, S. and Vassilenko, K.S. (1994) Determination of protein tertiary structure class from circular dichroism spectra. *Anal. Biochem.*, 222, 176–184.
- Wallace, B.A. (2000) Conformational changes by synchrotron radiation circular dichroism spectroscopy. *Nat. Struct. Biol.*, 7, 708–709.
- Whitmore, L. and Wallace, B.A. (2004) DICHROWEB, an online server for protein secondary structure analyses from circular dichroism spectroscopic data. *Nucleic Acids Res.*, 32, W668–W673.
- Winnig, M., Bufer, B. and Meyerhof, W. (2005) Valine 738 and lysine 735 in the fifth transmembrane domain of rTas1r3 mediate insensitivity towards lactisole of the rat sweet taste receptor. *BMC Neurosci.*, 6, 22.
- Xu, H., Staszewski, L., Tang, H., Adler, E., Zoller, M. and Li, X. (2004) Different functional roles of T1R subunits in the heteromeric taste receptors. *Proc. Natl Acad. Sci. USA*, 101, 14258–14263.
- Zhang, Y.H., Yan, X., Maier, C.S., Schimerlik, M.I. and Deinzer, M.L. (2002) Conformational analysis of intermediates involved in the *in vitro* folding pathways of recombinant human macrophage colony stimulating factor beta by sulfhydryl group trapping and hydrogen/deuterium pulsed labeling. *Biochemistry*, 41, 15495–15504.

Accepted March 17, 2006